The Immature Pediatric Appendicular Skeleton

Jie C. Nguyen, MD, MS[1,2] Dennis Caine, PhD[3]

[1] Department of Radiology, Children's Hospital of Philadelphia, Philadelphia, Pennsylvania
[2] Perelman School of Medicine at the University of Pennsylvania, Philadelphia, Pennsylvania
[3] Division of Education, Health and Behavior Studies, Kinesiology and Public Health Education, University of North Dakota, Grand Forks, North Dakota

Address for correspondence Jie C. Nguyen, MD, MS, Department of Radiology, Children's Hospital of Philadelphia, 3401 Civic Center Blvd., Philadelphia, PA 19104 (e-mail: nguyenj6@chop.edu).

Semin Musculoskelet Radiol 2024;28:361–374.

Abstract

Growth and maturation occur in a predictable pattern throughout the body and within each individual bone. In the appendicular skeleton, endochondral ossification predominates in long bones and growth plates. The ends of these long bones are sites of relative weakness in the immature skeleton and prone to injury from acute insult and overuse. We present the normal histoanatomy and physiology of the growth plate complex, highlighting the unique contribution of each component and shared similarities between primary and secondary complexes. Components of the growth plate complex include the physis proper, subjacent vascularity within the growth cartilage, and the ossification front. The second section describes imaging considerations and features of normal and abnormal growth. Finally, we review the Salter-Harris classification for acute fractures and offer examples of characteristic overuse injury patterns involving the epiphyseal (proximal humerus and distal radius), apophyseal (medial epicondyle and tibial tubercle), and secondary growth plate complexes (medial femoral condyle and capitellar osteochondritis dissecans). This article provides a foundation and basic framework to better understand and anticipate potential complications and growth disturbances and to ensure optimal follow-up and early intervention when treatment can be less invasive.

Keywords
- growth distrubance
- athlete
- fracture
- endochondral ossification
- growth plate

Growth and maturation from an osteochondral immature skeleton in children to the predominantly osseous mature skeleton in adults occurs in a predictable pattern throughout the body and within each bone. In flat bones, such as the calvarium, bone formation occurs directly on a mesenchymal scaffold, and is known as intramembranous ossification. In long bones that make up most of the appendicular skeleton, bone formation occurs on a cartilaginous framework called the growth plate (or physis), and this is known as endochondral ossification.[1,2] In children and pediatric athletes, traumatic and overuse injuries involving the appendicular skeleton are common, and the latter predominates. These injuries can lead to endochondral ossification dysfunction, producing a spectrum of findings that vary in severity and reversibility, impacting clinical symptomology and long-term outcomes.

During early embryonic development, around week 6 of gestation, the mesenchymal cells differentiate into chondrocytes, responsible for the formation of a cartilaginous model of the future skeleton. Within long bones, chondrocytes within the central portion of this cartilaginous anlage (future diaphysis) undergo cellular hypertrophy and the surrounding matrix calcifies. Around week 7 of gestation, the periosteal sleeve forms, and at the end of week 8, vascular invasion brings mesenchymal cells that differentiate into osteoblasts and osteoclasts.[3] Osteoblasts produce an osteoid matrix on the cartilaginous framework that later becomes the future primary ossification center. In contrast, the osteoclasts are

Issue Theme Pediatric Variants; Guest Editors, Jie C. Nguyen, MD, MS and Adam C. Zoga, MD, MBA

Thieme Medical Publishers, Inc., 333 Seventh Avenue, 18th Floor, New York, NY 10001, USA

DOI https://doi.org/10.1055/s-0044-1786151.
ISSN 1089-7860.

Fig. 1 Fetal bone anatomy. Sagittal TRUFI (True Fast Imaging with Steady-State Free Precession) magnetic resonance image from a 37-week gestational fetus shows ossified femoral shaft (arrowhead), cartilaginous epiphyses (arrows, femoral head and condyles), and apophysis (dashed arrow, greater trochanter) underlying the primary growth plates or physes (triangles). Wavy arrow denotes the cartilaginous patella.

responsible for bone remodeling and formation of the medullary cavity. These primary ossification centers grow and expand bidirectionally toward the ends of the long bone with the two leading edges becoming the proximal and distal primary growth plates[4,5] (►**Fig. 1**).

At the ends of these long bones, endochondral growth and ossification occur not only at the primary "discoid" growth plates that underlie epiphyses and apophyses, but also at the secondary "spherical" growth plates that surround epiphyses, apophyses, and small round bones, such as carpal, tarsal, and sesamoid bones. The pressure epiphyses (and the underlying epiphyseal growth plates) are subject to compressive forces, whereas the traction epiphyses or apophyses (and the underlying apophyseal growth plates) serve as attachment sites for tendons to bone and are primarily subject to tensile forces.

The smaller secondary growth plates (or acrophyses) are responsible for the centripetal growth of the underlying secondary ossification centers, which, depending on anatomical location, can be single or multiple and later coalesce as they slowly and progressively replace the unossified growth cartilage[1,83] (►**Fig. 2**). These primary and secondary growth plates are sites of relative weakness in the skeletally immature skeleton, especially during periods of rapid growth. Injury to the growth plate may produce a spectrum of clinical findings depending on the type of growth plate involved, anatomical location, which component or components are predominantly injured, the severity of the insult, and the patients' remaining growth potential.[6]

This article reviews the histoanatomy and unique contribution of each component of the growth plate complex, highlighting shared similarities between primary and secondary growth plates. Imaging considerations and imaging appearances of the growth plates at different stages of skeletal development and maturation are reviewed. Salter-Harris patterns of physeal fractures are then discussed briefly, followed by a more detailed review on our emerging understanding of the pathophysiology that underlies physeal stress injury, divided into those that involve the epiphyseal, apophyseal, and secondary growth plate complexes.

Representative examples with characteristic clinical presentations and key imaging findings that impact treatment

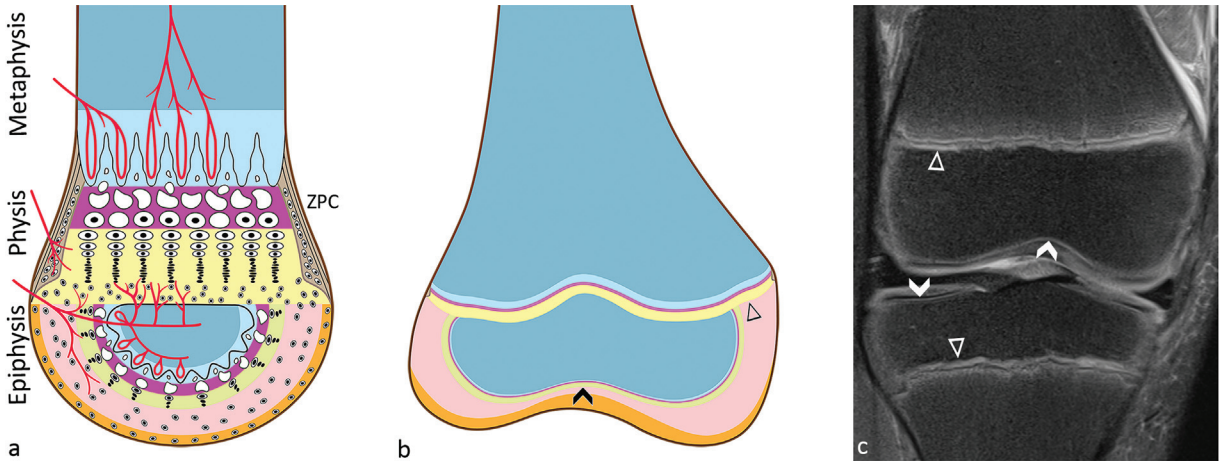

Fig. 2 Growth plate (physeal) anatomy. (**a**) Growth plate illustration shows arrangement of the primary and secondary physes, intact vascularity within the growth cartilage, and terminal vascular loops within the ossification front. Chondrocytes undergo apoptosis at and within the zone of provisional calcification (ZPC; shown in purple). (**b**) Distal femur illustration and (**c**) coronal intermediate-weighted fat-suppressed magnetic resonance image of the knee from a 10-year-old boy show primary (triangles) and secondary physes (chevrons). (a, b) Adapted and modified from Nguyen et al[6] with permission. Note: Illustrations are not drawn to scale.

Fig. 3 Example of endochondral ossification dysfunction. Anteroposterior radiograph (left) and coronal double-echo steady-state magnetic resonance (right) images from a 12-year-old female gymnast show asymmetric blunted growth across the distal radial physis, particularly worse along the ulnar side (arrows), with ulnar positive variance and early findings of acquired Madelung's deformity. Widening across the distal radioulnar joint (bracket) is present.

decision making are highlighted. An important goal of this article is to provide a foundation and basic framework to better understand and anticipate potential complications and growth disturbance arising from physeal stress injury, ensuring optimal follow-up and early intervention when treatment can be less invasive[6] (►**Fig. 3**).

Anatomy of the Growth Plate Complex

Growth plates are critical components of the immature skeleton. Impairment and dysfunction can produce lifelong morbidity, including limb-length discrepancy and angular deformity, resulting in altered joint biomechanics, compensatory secondary remodeling, and the risk for premature osteoarthritis.[7] Normal endochondral ossification requires not only zonal arrangement and proper cellular function of the physis proper but also intact vascularity on both sides of the physis. The epiphyseal growth plate complex includes the subjacent epiphysis and metaphysis (also known as the epiphyseal-physeal-metaphyseal complex).[8] The apophyseal growth plate complex includes the subjacent apophysis and metaphyseal-equivalent. The secondary growth plate complex includes the overlying unossified growth cartilage and the underlying secondary ossification center.

Injury to the growth plate proper (direct injury) and/or to the subjacent vasculature within the growth cartilage and newly formed ossification front (indirect injury) can lead to changes in the morphology of the growth plate and produce endochondral dysfunction, ranging from increased (overgrowth), to blunted (undergrowth), to complete cession of growth with subsequent premature physeal closure.[6] In the remainder of this article, for simplicity, we use *growth cartilage,* to denote the juxtaphyseal epiphysis, apophysis, and unossified growth cartilage, and *ossification front,* to denote the juxtaphyseal metaphysis, metaphyseal-equivalent, and secondary ossification center (SOC) bordering these primary and secondary growth plates.

Growth Plate Proper

On histology, the growth plate contains chondrocytes that mature as they move from the growth cartilage side toward the ossification front (►**Fig. 4**). Three distinct zones of chondrocytes are recognized, based on their microscopic cellular morphology, organization, and function: reserve, proliferative, and hypertrophic zones. The growth plate is surrounded at its periphery by the perichondrium (►**Fig. 2**).

Reserve Zone

In the reserve (or germinal) zone, chondrocytes are randomly distributed and only divide sporadically. An abundant surrounding extracellular matrix is responsible for storing nutrients, including glycogen and lipids. In this zone, collagen fibrils are disorganized.[4]

Proliferative Zone

In the proliferative zone, chondrocytes are organized into columns that divide rapidly. The top cell of each column (adjacent to the reserve zone) is the progenitor cell, and the rate of division correlates with the rate of bone growth. Less abundant extracellular matrix contains collagen fibrils organized into longitudinal septa. Oxygen and nutrients are derived from arterial branches that arise from the juxtaphyseal growth cartilage and travel within vascular channels and through the reserve zone to nourish the upper proliferative zone. Oxygen tension is the highest in this zone, facilitating robust aerobic metabolism and mitochondrial uptake of calcium.[4]

Hypertrophic Zone

In the hypertrophic zone, chondrocytes mature and undergo internal vacuolation and apoptosis (programmed cell death). This vacuolation process leads to the production of cytoplasmic "holes" and induces nuclear fragmentation and loss of cell membrane integrity. Extracellular glycogen is progressively depleted, and oxygen tension is substantially reduced, leading to anaerobic metabolism and mitochondrial release of calcium, facilitating matrix calcification.

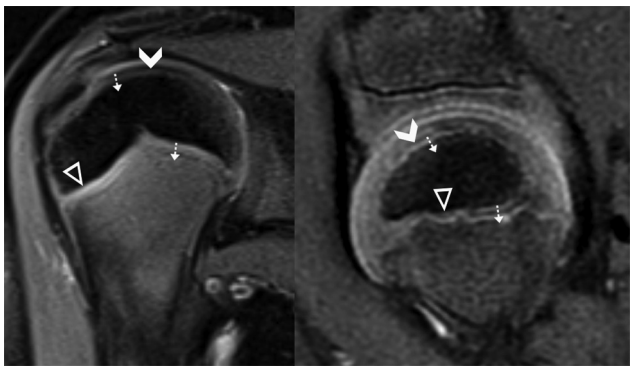

Fig. 4 Direction of chondrocyte growth on intermediate-weighted fat-suppressed magnetic resonance images. Coronal image of the shoulder from an 8-year-old girl (left) and sagittal image of the hip from a 3-year-old boy (right) show regional primary (triangles) and secondary physes (chevrons). Tiny dashed arrows denote direction of chondrocyte growth, maturation, and apoptosis.

Initially, calcification occurs along the longitudinal septa. Further accumulation of calcium salts creates amorphous deposits of calcium phosphate. These give way to hydroxyapatite crystals that subsequently coalesce, forming the zone of provisional calcification (ZPC). Progressive matrix calcification hinders the diffusion of nutrients and oxygen, further ensuring chondrocyte apoptosis. The ZPC demarcates the transition between the growth plate proper and the subjacent ossification front. In contrast to the arteries within the growth cartilage, the articular loops within the ossification front terminate just short of the ZPC and play no role in nourishing the hypertrophic chondrocytes.[3,4]

Perichondrium

The perichondrium surrounds the periphery of the growth plate and contains the groove of Ranvier and the ring of LaCroix. The groove of Ranvier is a wedge-shaped structure responsible for the transverse growth of the growth plate. The ring of LaCroix is a dense fibrous band that provides regional mechanical support to this osteochondral junction and is continuous with the periosteum.[1,4] Like the periosteum, the perichondrium is hypointense on all magnetic resonance imaging (MRI) pulse sequences. But in contrast to the periosteum, the perichondrium is tightly attached to the underlying growth plate. The perichondral vessels supply the perichondrium, which also nourishes the most peripheral aspects of the growth plate, leading to a relatively more vulnerable central growth plate that can be prone to ischemic insult and can produce a "cupping" deformity.[2]

Growth Cartilage: Epiphyses and Apophyses

With few exceptions, epiphyses and apophyses were initially entirely cartilaginous during fetal and early postnatal development. Nutrient vessels within growth cartilage travel within vascular channels, and small vascular branches extend into the growth plate proper to nourish chondrocytes within the reserve and upper proliferative zones.[4,9] These vessels produce a gradient of decreasing oxygen tension that extend from the growth cartilage side toward the ossification front side of the growth plate.

Disruption of these nutrient vessels leads not only to endochondral ossification dysfunction but also to epiphyseal and apophyseal deformity.[6,10] Scattered transphyseal vascular channels are present among infants $<$ 12 to 18 months of age that allows vascular communication and spread of disease to cross the growth plate.[11] But these vessels involute with progressive growth, and vascular communication is reestablished only after physeal closure at skeletal maturation.[12] This accounts for the relatively higher frequency of epiphyseal osteomyelitis among infants when compared with older children.[11]

Epiphyses

The immature osteochondral epiphysis contains a superficial layer of avascular articular cartilage, a middle layer of vascularized unossified growth cartilage, and a centrally located SOC. This middle growth cartilage layer is progressively replaced over time by the enlarging SOC, so that at skeletal maturation only the superficial layer of articular cartilage remains.

Apophyses

The immature osteochondral apophysis contains a peripheral layer of vascularized unossified growth cartilage and a centrally located SOC. Analogous to the epiphysis, this growth cartilage layer is progressively replaced over time by the enlarged SOC, so that at skeletal maturation no cartilage remains.

Secondary Ossification Centers

Within epiphyses and apophyses, the SOC initially forms following the coalescence of vascular channels centrally, which leads to the release of metalloproteinases (e.g., gelatinase B and collagenase 3) that break down the cartilaginous matrix, triggering chondrocyte hypertrophy, localized calcification, and ossification. The site of transient change within the regional cartilage, occurring just before the appearance of the SOC, is viewed as a pre-ossification center and should not be mistaken for pathology[5,13] (►**Fig. 5a**).

The newly formed SOC generally has a round morphology and is surrounded by a secondary growth plate that has the same zonal arrangement as the primary growth plate but is smaller in size. As growth continues, portions of the secondary growth plate close at sites where the overlying growth cartilage has been depleted. This results in the SOC losing its initial spherical morphology and conforming to its underlying cartilaginous framework. For example, in the femoral condyles, the portion of the secondary growth plate that faces the primary growth plate closes first, producing a semicircular morphology of the SOC[4,5] (►**Fig. 2**).

It is also common for some epiphyses and apophyses to have multiple smaller SOCs that coalesce over time, commonly observed in the immature proximal humeral head, trochlea of the distal humerus, and tibial tuberosity of the

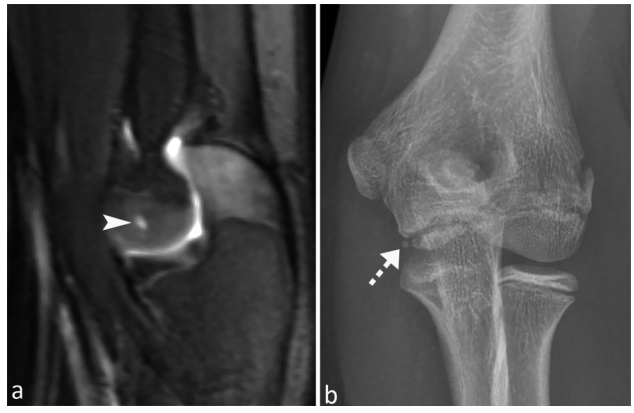

Fig. 5 Spectrum of normal ossification involving the immature trochlea. (**a**) Sagittal T2-weighted fat-suppressed magnetic resonance image from a 6-year-old boy shows the normal appearance of a hyperintense pre-ossification center (arrowhead). (**b**) Anteroposterior radiograph from a 13-year-old boy shows fragmented and heterogeneously sclerotic appearance of the trochlear ossification (dashed arrow).

proximal tibia. In the humeral head, for example, three (medial head, greater and lesser tuberosity) SOCs coalesce at early childhood to form an irregularly shaped SOC that ultimately become the humeral head.[14]

Trochlear ossification is well recognized as one of the most widely variable and irregular, and is occasionally mistaken for pathology (►**Fig. 5b**). However, the bilateral appearance of this finding and the lack of localized symptoms are helpful signs to avoid unintentional false-positive diagnoses.[15] Similarly, intra-cartilaginous trochlear tuberosity ossification must be distinguished from Osgood-Schlatter disease and pathologic avulsion fracture. These are described further in the other anatomically designated articles within the current issue of *Seminars.*

Ossification Front: Metaphyses, Metaphyseal-Equivalents, and SOCs

At the primary spongiosa of the juxtaphyseal metaphysis and metaphyseal-equivalent location, and at the peripheral margin of SOCs that abut the ZPC, osteoblasts lay down bone on the calcified cartilaginous bars. Regional vasculature forms terminal vascular loops and capillary tufts that terminate just proximal to the ZPC, ensuring anaerobic metabolism within the adjacent hypertrophic zone of the growth plate proper, facilitating and indirectly ensuring chondrocyte apoptosis[3,4] (►**Fig. 2**). Disruption of these vessels hinders chondrocyte removal and regional bone formation, leading to physeal widening.

Metaphyses and Metaphyseal-Equivalents

Newly formed bone is remodeled within the secondary spongiosa. Internal remodeling entails the removal of cartilaginous bars and the replacement of lamellar bone, whereas external remodeling involves the peripheral reshaping of the metaphysis into its final funnel-shaped morphology.[3,4] Regional blood supply is derived from a combination of centrally located branches that originate from the diaphyseal nutrient artery and peripherally located vessels that penetrate the metaphysis and contribute $\sim$ 80% and $\sim$ 20% to the regional blood supply, respectively.[16]

Secondary Ossification Centers

Newly formed SOC contains hematopoietic red marrow that converts to fatty yellow marrow at $\sim$ 6 months after its formation. As the SOC grows along its peripheral margin (ossification front), marrow conversion proceeds in the same central-to-peripheral direction.[17] This difference in cellular composition is reflected in the change in signal intensity on MRI that must be distinguished from superimposed insult. Latter pathologic marrow edema is more focal and centered over the site of pathology. Normal physiology marrow conversion and reconversion is further discussed in the section, under growth-related imaging features.

Imaging Considerations and Features

At birth, the growth plates are relatively smooth and flat. With progressive growth, undulation of the growth plate can be observed and is believed to be in response to regional anatomy and location-dependent physiologic dynamic biomechanical forces.[12,18] During early childhood, the thickness of the growth plate remains relatively constant because of an intricate balance between chondrocyte proliferation and apoptosis. Narrowing across the growth plate signals its impending closure and upcoming regional skeletal maturation. Closure starts at sites of major undulation that differs between growth plates depending on anatomical location. The final conversion of chondrocytes into bone leaves behind a physeal scar that represents residual ZPC or leftover horizontal trabeculae.[2] This physeal scar is slowly remodeled and finally disappears by early adulthood.[19]

Imaging Modalities

Different imaging modalities can be used to evaluate and monitor for growth disturbance, but the precise approach depends on the patient's age, skeletal maturity, and clinical question. Imaging is routinely used to confirm and characterize a clinically suspected diagnosis, and to exclude alternative diagnoses. It generally begins with screening radiographs, followed by advanced cross-sectional imaging to further characterize regional anatomy and pathology, and to estimate growth potential, as well as to help guide treatment planning. This section provides an overview of the technical considerations for each of the commonly clinically used imaging modalities: radiographs, MRI, computed tomography (CT), and musculoskeletal ultrasonography (US).

Radiographs

Although the cartilaginous growth plates are radiolucent, radiography remains the initial imaging modality of choice because it is readily available and can exclude alternative diagnoses. Radiographs are generally obtained in two (anteroposterior or posteroanterior and lateral) or three (additional oblique) views, depending on the anatomical location and clinical concerns. Additional oblique and stressed views, as well as single or multiple views of the contralateral asymptomatic side, may be helpful in ambiguous cases to detect subtle asymmetric physeal widening, early remodeling, and/or premature physeal closure (►**Fig. 6**). Full-length long bone or limb radiographs provide an overview of the regional osseous anatomy, and serial examinations are often used to monitor for asymmetric growth, development of angulation deformity, and response to intervention.

Computed Tomography

As with radiographs, the cartilaginous growth plate is hypoattenuating, and its presence is only indirectly inferred from the subjacent ossified elements. In the very young, the abundance of unossified growth cartilage cannot be reliably distinguished from the cartilaginous physis. CT is less routinely used among children due to concerns about the potential adverse cumulative effects of ionizing radiation on growing tissue and the abundance of radiolucent cartilage. The main indications for using CT to assess regional physeal anatomy and pathology include a suspected small

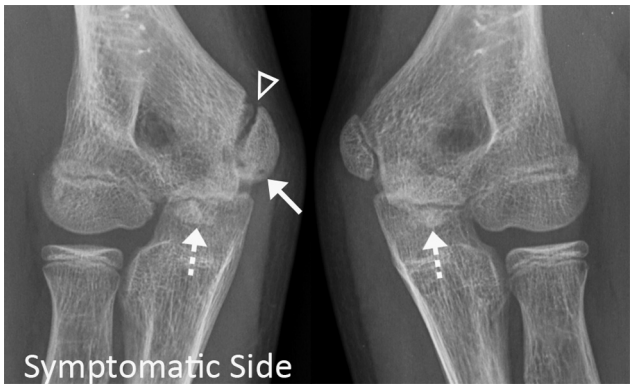

Fig. 6 Primary stress injury (PSI) involving the medial epicondylar apophysis. Oblique radiographs from the symptomatic (left image) and asymptomatic comparison elbows (right image) show stereotypical findings of overuse with asymmetric physeal widening (triangle), sclerosis, fragmentation, and overgrowth of the symptomatic medial epicondyle (arrow). Note the normal irregular and sclerotic normal appearance of the trochlear ossifications bilaterally (dashed arrows).

transphyseal osseous bar or tethering, physeal fractures with intra-articular extension, preoperative planning and/or need for intraoperative navigation, and for those patients who are contraindicated for MRI or sedation.

Magnetic Resonance Imaging

MRI is the preferred imaging modality for the comprehensive evaluation of hyaline cartilage, bone marrow signal intensity, and surrounding soft tissues without the use of ionizing radiation (►**Fig. 7**). The main drawbacks are possible need for patient sedation, limited immediate availability, and higher cost. Hyaline cartilage is mainly composed of water and a solid matrix that consists of primarily type II collagen and large aggregating proteoglycan macromolecules. Therefore, hyaline cartilage is isointense on T1-weighted images and hyperintense on fluid-sensitive images (e.g., T2-weighted fat-saturated, short tau inversion recovery, STIR) when compared with the signal intensity of skeletal muscle.

Articular, growth, and growth plate cartilage are different types of hyaline cartilage and distinguished based on their anatomical location and signal intensities on fluid-sensitive and contrast-enhanced MRI pulse sequences.[2,20,21] Cartilage-sensitive pulse sequences such as gradient-recalled echo (GRE) and double-echo steady-state (DESS) images facilitate excellent contrast between the bright cartilage and the dark bone. They can identify and estimate percentage of growth plate closure that directly impacts treatment planning.[22,23] Although small and centrally located transphyseal bridges in children near skeletal maturity can be treated conservatively, larger, multifocal, and/or eccentrically located bridges in younger skeletally immature children will require serial imaging and potentially surgical intervention[6] (►**Fig. 8**).

Musculoskeletal Ultrasonography

Cartilage is hypoechogenic on US, but distinction between articular, growth, and growth plate cartilage is not possible and only inferred based on their expected anatomical location. At birth, the diaphyses and metaphyses are ossified, preventing further sonographic penetration. However, the epiphyses and apophyses vary in composition, depending on anatomical location, ranging from completely cartilaginous to partially ossified. Partially ossified epiphyses and apophyses allow variable sonographic penetration that is greater among younger children with smaller body parts and more unossified cartilage. Contralateral comparison, multifocal assessment, and dynamic assessment are possible with US and without the need for patient sedation, making it an ideal complementary imaging modality of choice among younger children. The main drawbacks of US are operator dependence and the current lack of consensus protocols for imaging.[11]

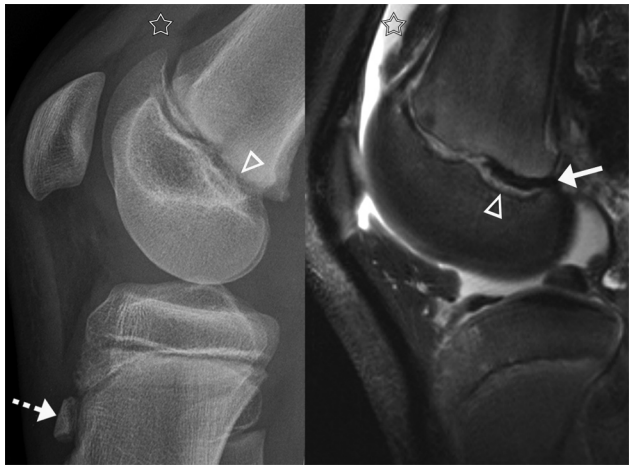

Fig. 7 Distal femur physeal fracture. Lateral radiograph (left image) and corresponding sagittal T2-weighted fat-suppressed magnetic resonance (right image) image show subtle asymmetric widening of the distal femoral physis (triangles) from Salter-Harris type I fracture with posterior periosteal interposition (arrow). A joint effusion is present (stars). A normal immature tibial tubercle apophyseal ossification is noted (dashed arrow).

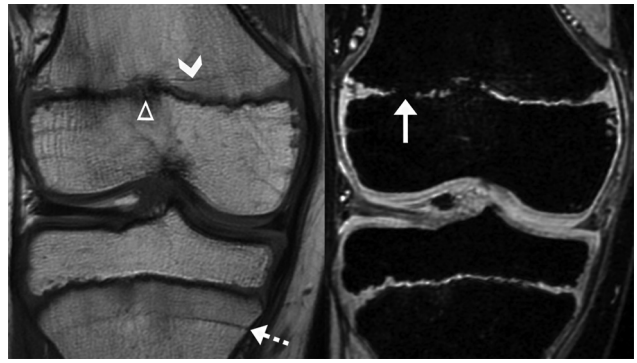

Fig. 8 Normal and abnormal growth recovery lines in the setting of transphyseal tethering. Coronal T1-weighted (left) and three-dimensional multiple echo recombined gradient echo magnetic resonance (right) images from a 10-year-old boy, 1 year after a displaced Salter-Harris type II distal femur fracture, show physeal irregularity (triangle), scattered foci of transphyseal tethering (arrow), and an abnormally angled growth recovery line (chevron). For comparison, a normal growth arrest line (dashed arrow) is identified within the proximal tibia.

Growth-Related Imaging Features

Unique features of the immature skeleton commonly encountered during clinical practice are laminar growth plate appearance, growth recovery lines, transphyseal tethering, normal patterns of physiologic marrow conversion, and stress-related reconversion.

Laminar Growth Plate Appearance

The bilaminar appearance of the growth plate proper on fluid-sensitive MRI includes the hyperintense cartilaginous portion and the hypointense thinner band of ZPC. On higher spatial resolution MRI, a trilaminar appearance of the growth plate can be observed, typically underlying the larger epiphyses. This is due to a third, less well-defined hyperintense layer, located at the ossification front of the primary spongiosa, abutting the ZPC and containing a few residual chondrocytes, just before complete replacement by bone. Due to the relatively smaller size of the secondary growth plates, only a bilaminar appearance is typically observed (►**Figs. 2** and **4**).

Growth Recovery Lines

Growth recovery lines (also known as growth arrest lines) represent thickened, horizontally oriented trabeculae that form because of a temporary slowdown of longitudinal growth during a time of stress. These lines are surrogate markers that exclude premature physeal closure. They are thickest and most obvious when they are newly formed and within more rapidly growing ossification fronts, such as those found in the bones of the distal forearm and around the knee joint. Over time, these lines are displaced toward the diaphysis and finally disappear with progressive bony remodeling.

Symmetrical growth results in lines that parallel the contour of their respective growth plates. Angled or obliquely oriented growth recovery lines indicate underlying endochondral ossification dysfunction, potential tethering, and/or progressive acquired angulation deformity (►**Fig. 9**). Isolated growth recovery lines in the fibula or the ulna indicate an increased possibility of diffuse premature growth plate closure of the ipsilateral tibia and radius, respectively. Growth recovery lines are typically hypointense on all MRI images and best visualized against a background of hyperintense yellow marrow on non–fat-saturated images (►**Fig. 8**). MRI outperforms radiographs in the earlier detection of these lines by 6 to 7 weeks.[6,24]

Transphyseal Tethering

Heterogeneous signal intensity and irregular morphology of the growth plate proper can suggest endochondral ossification dysfunction and precede premature physeal closure that can be focal or diffuse. Transphyseal tethering can be osseous or fibrocartilaginous (nonosseous), and the latter can be missed on radiographs and CT.[25] Thus MRI is the preferred imaging modality for the diagnosis and estimation of clinically-suspected transphyseal bridge, helping to guide treatment decision making. Large osseous sites of tethering often contain fatty marrow signal intensity and thus are best depicted on T1-weighted images. In contrast, small bony and nonosseous sites of tethering can have variable signal intensity and may be uncovered owing to the presence of adjacent bone marrow edema produced in response to relatively increased regional tissue rigidity.[26]

Although radiographs are helpful in the initial screening of premature physeal closure and serial monitoring of asymmetric growth, they should not be used to estimate the underlying severity or extent of transphyseal tethering, which can be overestimated on radiographs in more than a third of cases when compared with MRI.[27] Finally, these pathologic sites of tethering should not be confused with a focal periphyseal edema (FOPE) zone that occurs at stereotypical sites of early physiologic growth plate closure.[6,28] These FOPE zones are best studied and further described in the article on the pediatric knee in this issue.

Bone Marrow Conversion and Reconversion

Normal marrow signal intensity changes with growth, maturation, and in response to stress. A comprehensive review of the pediatric marrow is beyond the scope of this article but has been previously described.[29] Briefly, on MRI, signal

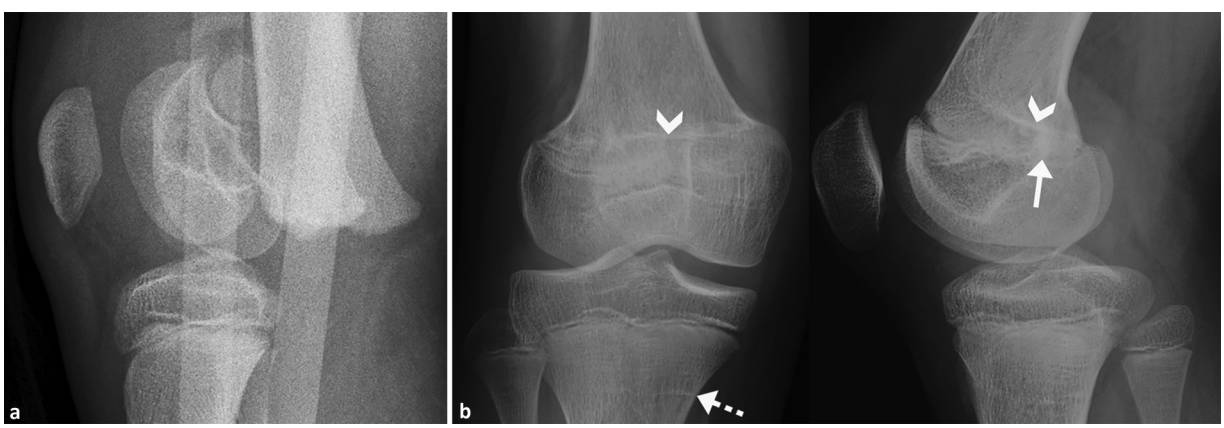

Fig. 9 Growth disturbance with asymmetric growth. (**a**) Lateral radiograph shows a displaced Salter-Harris type II distal femur fracture in a 9-year-old boy, imaged with an external immobilizer in place. (**b**) Follow-up anteroposterior and lateral radiographs, obtained 2 years later, show posterior physeal closure (arrow), producing asymmetric growth across the distal femur and an angled growth arrest line (chevrons). Note the normal, almost completely reabsorbed faint growth arrest lines identified within the proximal tibial metaphysis (dashed arrow).

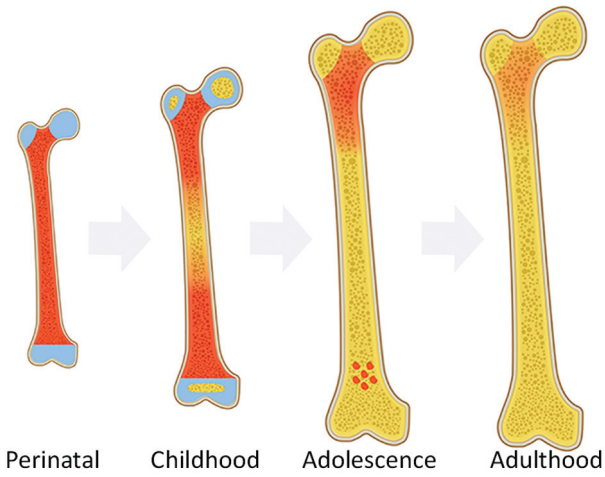

Fig. 10 Illustration of normal sequence of marrow conversion within a long bone (femur). In the pre- and perinatal period, red marrow (red) predominates within the ossified diaphyses and metaphyses while the epiphyses and apophyses remain completely or predominantly cartilaginous (blue). During early childhood, marrow conversion to yellow marrow (yellow) starts within the mid-diaphysis and progresses bidirectionally toward the metaphyses, slightly faster distally than proximally, so that in late adolescence and throughout adulthood, red marrow is mostly found clustered within the proximal metaphyses. Illustration adapted and modified from Chan et al[29] with permission.

intensity of normal marrow reflects a combination of the distribution of marrow elements (hematopoietic red and fatty yellow marrow) and regional marrow edema. Physiologic conversion from red to yellow marrow occurs throughout life but at a more rapid pace during childhood. In long bones, marrow conversion starts in the mid-diaphysis and bidirectional conversion extends toward the metaphyses, slightly faster in the distal than the proximal metaphyses. By skeletal maturity and early adulthood, residual red marrow is mostly observed within the axial skeleton and proximal metaphyses of the appendicular skeleton (►**Fig. 10**).

In children who experience systemic stress, marrow reconversion from yellow back to red marrow occur in the exact and opposite direction from normal physiologic conversion. This reconversion starts within the metaphyses and progresses toward the diaphysis, epiphyses, and apophyses. At ~ 6 months after the appearance of the SOC, marrow signal intensity follows that of yellow marrow. Thus when signal intensity within the epiphyses and apophyses is lower than that observed within the subjacent metaphyses, pathologic marrow must be suspected.[17] Imaging features that favor red marrow over pathologic marrow replacement or infiltration include higher signal intensity relative to skeletal muscle (due to intrinsic fatty elements), feathery margins that interdigitate with adjacent yellow marrow, relative bilaterality, and absence of mass effect.[29]

Acute Physeal Fracture

Growth plates are two to five times weaker than the surrounding soft tissues, making them the "weak link" and prone to injury.[30] The primary growth plates underlying pressure epiphyses are the best studied in the published literature, and ~ 18% of all pediatric fractures involve the growth plate with the peak incidence of these fractures overlapping with the adolescent growth spurt.[31,32] This overlap is postulated to be the result of a combination of factors, such as temporary bone fragility where longitudinal growth outpaces bone mineralization, the ability to generate greater force, and the involution of the perichondral sleeve that stabilizes the osteochondral interface.[14,33–35] Moreover, the relatively lower stiffness of the hypertrophic chondrocytes, in combination with their large size, renders them particularly vulnerable to injury from excessive mechanical loading.[36]

The Salter-Harris classification of physeal fractures remains the system most widely used clinically for describing these fractures. Type I fractures are uncommon, accounting for < 10% of growth plate fractures, and transverse fracture cleavage planes are centered within the growth plate. Type II fractures are most common, accounting for about three quarters of growth plate fractures, and fracture cleavage planes involve the metaphysis. Types III and IV fractures are uncommon intra-articular fractures that involve the epiphysis, or both the epiphysis and metaphysis, respectively. These latter fractures often require preoperative CT to determine precise fracture alignment and the need for surgical reduction. Relatively rare type V fractures, postulated to involve compression injury, are only diagnosed retrospectively after the development of growth disturbance.[6,19,26]

Physeal Overuse Injury

In contrast to high-energy acute insults that often lead to fractures and/or dislocations, the growing participation in pediatric sports with higher intensity training and earlier specialization has led to increased rates of overuse injuries that result from repetitive microtrauma at submaximal stress.[37] It is postulated that in these skeletally immature athletes, this stress initially and predominantly temporally compromises vascular perfusion within the ossification front, leading to prolonged survival of hypertrophic chondrocytes and lengthening of the fragile chondrocyte columns, producing growth plate widening.[38,39]

Laor and colleagues[40] originally proposed two distinct patterns of chondrocyte extension into the ossification front: a focal "tongue" of persistent cartilage from focal vascular insult versus a "broad band" from a more diffuse insult. The latter diffuse pattern is more commonly encountered among these pediatric athletes.[41] This pattern carries an overall favorable prognosis and is often reversible if diagnosed and treated early, allowing restoration of regional perfusion.[8] However, if undiagnosed or if the patient is noncompliant with conservative treatment, the biomechanically relatively weaker osteochondral junction is vulnerable to additional insults and stresses, increasing the risk for progressive injury that can affect the growth plate proper and adjacent growth cartilage, which is less reversible and can lead to permanent growth disturbance[8,41] (►**Fig. 3**).

The following section discusses our emerging understanding of the pathophysiology that underlies physeal

stress injury, divided into those injuries that involve the epiphyseal, apophyseal, and secondary growth plate complexes.

Epiphyseal Growth Plate Complex

The epiphyseal growth plate complexes, including the primary growth plate proper and subjacent epiphysis and metaphysis, are found at one or both ends of a long bone. For the smaller long bones of the hands and feet (e.g., metacarpals, metatarsals, and phalanges), this complex is found at only one end, whereas for the larger long bones of the appendicular skeleton (e.g., humeri and femurs), this complex is found at both ends of the bone. In the latter larger long bones, the proximal and distal epiphyseal physes often have differential growth rates and thus do not contribute equally to the final length of the underlying bone.

For example, ~ 71% of femoral and 57% of tibial lengthening occur at the distal femoral and proximal tibial primary physes, which account for ~ 37% and 25% of the overall total length of the lower extremity, respectively.[42,43] This information is critically important because it impacts the potential for regional remodeling and severity of the resulting growth disturbance[44] (►**Fig. 2**). The best studied examples of overuse injury that involve the epiphyseal growth plate complex include the proximal humerus among overhead throwing athletes and the distal radius among gymnasts and platform divers.[7]

Proximal Humeral Epiphyseal Physeal Complex

Among baseball pitchers, a high level of external rotational torque is placed on the proximal humerus during the late cocking phase of a pitch.[45] This repetitive microtraumatic sheer, torque, or traction on the proximal humeral physeal complex is postulated to damage the most susceptible vertically oriented collagen fibers within the hypertrophic zone and subjacent vascularity within the newly formed bone of the metaphyseal ossification front.[14,34] Suboptimal throwing technique, excessive throwing volume, high throwing speeds, and playing breaking pitches (e.g., curveballs) can all predispose this physeal complex to cumulative stress and injury.[14] These athletes present with pain during overhead activities that worsen during throws and on physical examination; tenderness is centered over the proximal humerus.[46]

Imaging assessment starts with radiographs, which should include an external rotation view that profiles the anterolateral aspect of the humeral physis, the most common site of early injury.[47] Radiographic findings include growth plate widening, indistinctness or loss of ZPC (reflecting active disease), irregularity and sclerosis within the subjacent metaphysis (reflecting chronicity).[14] Physiologic growth plate closure starts centrally and progresses in a centripetal fashion toward the periphery, with a slight delay in closure along the lateral physis that should not be mistaken for pathology.[47] These findings can be subtle, and comparison views of the contralateral asymptomatic shoulder can improve diagnostic accuracy and reader confidence. MRI findings mirror radiographic findings, and the presence of subjacent marrow edema suggests active ongoing injury[34] (►**Fig. 11**).

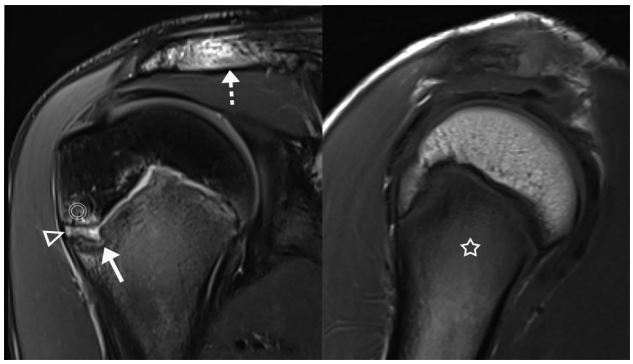

Fig. 11 Primary stress injury (PSI) involving the proximal humeral epiphysis. Coronal T2-weighted fat-suppressed (left) and sagittal T1-weighted magnetic resonance (right) images from a 13-year-old male baseball pitcher show stereotypical findings of overuse injury with asymmetric physeal widening, more severe laterally (triangle), subjacent marrow edema (circle), and metaphyseal sclerosis (arrow). Red marrow hyperplasia is identified within the proximal humeral metaphysis (star). Acromion marrow edema (dashed arrow) is also present.

Distal Forearm Epiphyseal Physeal Complexes

Among gymnasts, repetitive compressive and rotational forces are placed on the distal forearm that preferentially affects the distal radius over the distal ulna because the former has a greater cross-sectional area and is responsible for the bulk of the load transmission across the wrist joint.[41,48] These athletes typically present with localized pain and tenderness centered over the distal forearm, often without a history of acute trauma. Symptoms increase with load-bearing activities and are relieved with rest.

Imaging assessment begins with radiographs where findings of overuse injury are observed and can be limited to the distal radius or involve both the distal radius and ulna.[19] In contrast to baseball pitchers where findings are often limited to the dominant throwing arm, findings among these gymnasts are usually bilateral, but one side may be worse and more symptomatic than the other.[41,49]

MRI findings of overuse injury are often observed, and again marrow edema suggests an active ongoing insult. When early intervention is successful, healing occurs with centripetal ossification of the metaphyseal cartilage, leading to normalization of the growth plate width and reconstitution of the ZPC.[6,40,50] However, ongoing stress and recurrent injury can lead to irreversible damage, resulting in stunted growth and long-term deformity.[8,48,51] This latter observation is postulated to account for the higher prevalence of ulnar positive variance among gymnasts[41,52] (►**Fig. 3**).

Apophyseal Growth Plate Complex

Apophyses contribute to the morphology at the distal ends of mature bone and serve as attachment sites for tendons and ligaments. Analogous to the epiphyseal primary physes, apophyseal primary physes are weaker than the attaching soft tissues and thus prone to failure that can present as acute avulsion fractures and overuse injuries. The latter apophysitis is underrecognized and underdiagnosed, often incidentally discovered after an acute injury. It is postulated that cumulative submaximal repetitive stresses weaken the

already venerable osteochondral junction, requiring less energy to produce a frank fracture.[8] The best studied examples of apophyseal injuries include the medial epicondyle among overhead throwers and tibial tubercle among athletes who perform repetitive kicking and jumping (quadriceps contraction) motions.[53]

Medial Epicondyle Apophyseal Physeal Complex

Repetitive valgus stress across the elbow can produce a spectrum of findings (also known as thrower's elbow). The most frequent site of injury involves the medial elbow. Among skeletally immature athletes, medial epicondyle apophysitis is common, whereas among skeletally mature athletes, soft tissue (ulnar collateral ligament and flexor-pronator mass) injuries predominate.[54,55] Patients typically present with medial elbow pain that worsens with throwing.

Imaging assessment again starts with radiographs, which can be normal, and findings may be relatively subtle. But in those immature athletes with prolonged symptoms, findings of overuse injury can include growth plate widening, fragmentation of the medial epicondyle ossification, and regional sclerosis. Medial epicondyle overgrowth from regional hyperemia can occur, leading to advanced skeletal maturation[56] (►**Fig. 6**).

Superimposed avulsion fractures can either include the entire medial epicondyle apophysis (centered at the primary physis) or only the distal epicondyle that underlies the attachment of the ulnar collateral ligament (centered at the secondary physis).[54] MRI is preferred over CT for its overall more comprehensive assessment of the elbow, including the presence of marrow edema (that suggests ongoing active stress) (►**Fig. 12**), integrity of ulnar collateral ligament and flexor-pronator mass, and any findings of internal derangement within the elbow, such as osteochondritis dissecans (OCD),[57,58] further discussed in the section on the secondary growth plate complex.

Tibial Tubercle Apophyseal Physeal Complex

Tibial tubercle develops in four stages: cartilaginous, apophyseal, epiphyseal, and osseous stages. The first cartilaginous stage (at approximately < 8 years of age in girls and < 9 years in boys) exists before the appearance of the secondary ossification centers. During the second, apophyseal stage ($\sim$ 8–12 years of age in girls and 9–14 years in boys), ossification centers appear, enlarge, and coalesce, whereas during the third epiphyseal stage ($\sim$ 10–15 years of age in girls and 11–17 years in boys), the maturing apophyseal ossification coalesces with the proximal tibial epiphyseal ossification. The final osseous stage (approximately > 15 years of age in girls and > 17 years in boys) is reached after complete physeal closure at skeletal maturity.

The transition from fibrocartilage to columnar physeal cartilage and ultimate physeal closure occur in a proximal to distal direction, predisposing tissue at the distal end of the tibial tubercle to differential stress and the risk for biomechanical failure, particularly near skeletal maturation.[59] Currently, there is no consensus regarding whether or not overuse injury (e.g., Osgood-Schlatter disease) predisposes patients to avulsion fractures, but both processes share the same culprit mechanism of forceful quadriceps contraction (often associated with kicking, sprinting, or jumping) transmitted to the immature tibial tubercle by the attaching patellar tendon.[60–62]

Osgood-Schlatter disease is generally a clinical diagnosis and patients are treated conservatively.[63] But in those with atypical symptoms or concern for superimposed avulsions, imaging assessment starts with radiographs. In contrast to Osgood-Schlatter disease with typical radiographic findings of tibial tubercle fragmentation, distal patellar tendinosis, and/or overlying soft tissue edema,[59] tibial tubercle fractures are characterized by fracture extent that can be limited to the anterior cortex of the tuberosity or involve the apophyseal growth plate, epiphyseal growth plate, and extend into the knee joint and/or the posterior proximal tibial metaphysis[61,62] (►**Fig. 13**). MRI is preferred over CT, particularly for those patients with intra-articular extension, to detect internal derangement, soft tissue injury, and/or entrapment.[59,62] Rare complications include growth arrest with genu recurvatum and limb-length discrepancy, particularly among those who have sustained injury at a younger age.[61,62]

Secondary Growth Plate Complex

The secondary growth plates are responsible for the enlargement of the secondary ossification centers. These peripherally located growth plates grow in a centripetal direction, slowly and progressively replacing the overlying unossified

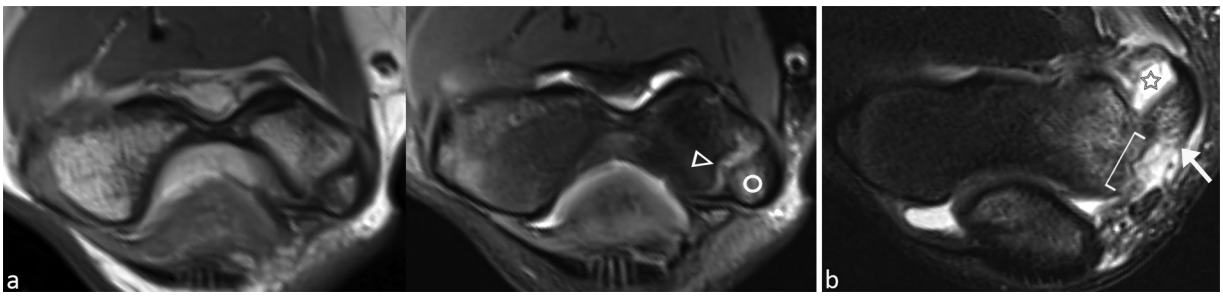

Fig. 12 Examples of apophyseal primary periphyseal stress injury (PPSI) and avulsion fracture of the medial epicondyle. (**a**) Axial intermediate-weighted (left) and T2-weighted fat-suppressed MR (middle) images from a 9-year-old boy show irregularity and widening of the medial epicondyle physis (triangle) and surrounding reactive marrow edema (circle). (**b**) Axial T2-weighted fat-suppressed MR (right) image from a different 12-year-old boy shows anterior displacement of the avulsed medial epicondyle (arrow) from its donor site (bracket) with more intense reactive marrow edema and an elbow effusion (star).

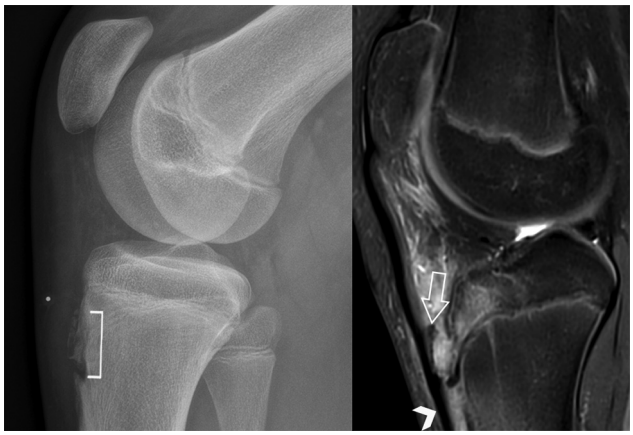

Fig. 13 Tibial tuberosity avulsion fracture. Lateral radiograph (left) from a 12-year-old boy shows irregularity and fragmentation of the anterior distal tibial tuberosity (bracket) and overlying soft tissue swelling that underlie the skin marker (dot). Sagittal T2-weighted fat-suppressed MR (right) image, obtained 2 weeks later for worsening pain, shows a linear avulsed fragment (block arrow), underlying the patellar tendon and distal periosteal stripping (chevron).

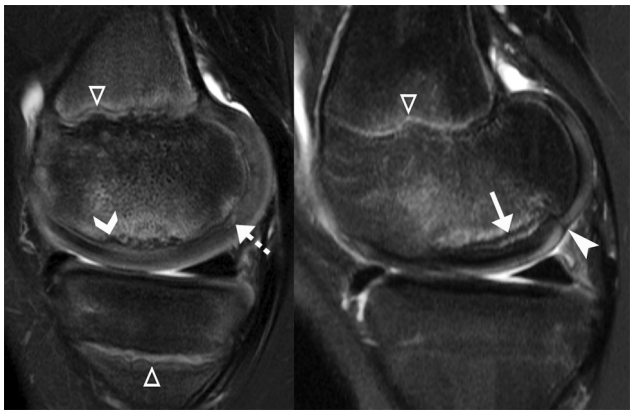

Fig. 14 Examples of stable and unstable medial femoral condyle juvenile osteochondritis dissecans (JOCD) lesions. Sagittal T2-weighted fat-suppressed image from an 11-year-old boy (left) shows a stable JOCD with irregularity of the ossification front (chevron), perilesional marrow edema, and intact overlying cartilage. A normal ossification variant is identified within the posterior femoral condyle (dashed arrow). In contrast, sagittal T2-weighted fat-suppressed image from a 14-year-old girl (right) shows an unstable JOCD with focal hypointense full-thickness chondrosis (arrowhead) and disruption of the radius of curvature. Other findings include high (but not fluid-high) signal intensity interface, marginal sclerosis of the parent bone (arrow), and perilesional marrow edema. Note the open regional physes (triangles) reflecting skeletal immaturity of the 11-year-old boy and impending maturity of the 14-year-old girl.

growth cartilage.[1] It is postulated that injury to the secondary growth plate complex may be the pathophysiologic mechanism that underlies the development of OCD[64] (►**Fig. 2**).

OCD is one of the leading causes of chronic knee pain among children and young adults.[65] The medial femoral condyle is the most common anatomical location throughout the body and within the knee, thus, the best studied. OCD lesions were classically divided into juvenile (JOCD) and adult lesions according to whether the regional growth plates are open or closed at the time of diagnosis. This is important because whereas symptomatic adult lesions rarely heal spontaneously, patients with JOCD are commonly asymptomatic, and more than half can heal with conservative management.[66–70] This latter observation has been attributed to the presence of vascularized unossified growth cartilage among skeletally immature children, providing an opportunity for self-repair and healing.[9]

Radiographic findings include focal subchondral lucency, marginal sclerosis, progeny mineralization, fragmentation, and/or intra-articular bodies. MRI is the preferred next imaging modality of choice to characterize lesion stability and to monitor treatment response, helping optimize the decision and timing for surgical intervention. Although several MRI features have been proposed,[68,71,72] in the knee, the most clinically used criteria are the presence of an osteochondral defect (empty crater), overlying chondrosis, disruption of the radius of curvature, fluid-like high signal intensity at the interface, cysts (circumferential or a single cyst > 5 mm), and/or multiple breaks in the subchondral bone plate[72,73] (►**Fig. 14**).

Less commonly, OCD lesions are found within the elbow joint that disproportionately involve the capitellum,[74,75] particularly among baseball pitchers and gymnasts. Repetitive valgus overload with the elbow in flexion is believed to cause these lesions among baseball players, whereas weight bearing with the elbow in extension may be the cause among gymnasts.[76] Histopathologic analysis previously showed that compressive forces can cause focal endochondral ossification dysfunction at these physiologically active, peripherally located secondary physes.[64,77–79]

In contrast to medial femoral condyle lesions, capitellar OCD lesions are more likely to be unstable at the time of diagnosis, but it is uncertain whether this is due to either or to a combination of regional differences (more tenuous regional blood supply within the distal humerus)[80,81] or delayed clinical presentation (►**Fig. 15**). On MRI, although the presence of an osteochondral defect, intra-articular body, overlying cartilage changes, subchondral bone plate disruption, and hyperintense rim at the interface were significantly more common among unstable lesions, the number or size of the perilesional cysts did not significantly differ between stable and unstable capitellar OCD when arthroscopy was used as the reference standard.[82]

Regardless of the anatomical location, treatment for OCD depends on lesion stability. Stable lesions are treated conservatively, but unstable lesions or lesions that have failed a trial of conservative therapy, particularly in those who have reached skeletal maturity, are often treated surgically to prevent further joint damage and reduce the risk for future premature osteoarthritis.[82]

Summary

Growth and maturation occur in a predictable pattern, and endochondral ossification predominates within long bones of the appendicular skeleton, occurring in both primary and secondary growth plate complexes. These growth plate

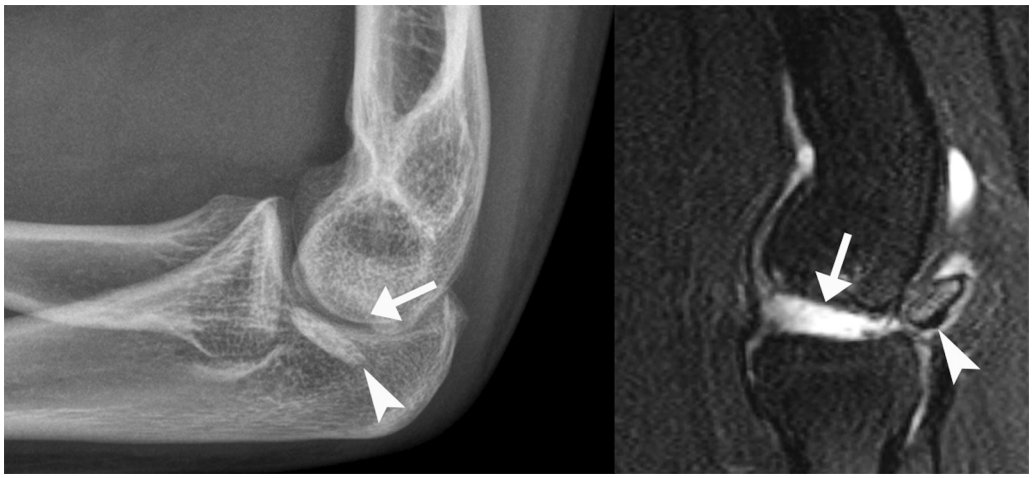

Fig. 15 Example of unstable capitellar osteochondritis dissecans with empty crater and displaced progeny. Lateral radiograph (left) and sagittal T2-weighted fat-suppressed magnetic resonance (right) images from a 13-year-old female gymnast with long-standing elbow pain show an empty crater (arrows) and an ossified intra-articular body (arrowheads). Regional physes have closed, reflecting skeletal maturity.

complexes are sites of relative weakness, especially during pubescence, and they are at risk for acute insult or overuse injuries. A basic knowledge of the normal histoanatomy and physiology of the growth plate complex ensures an improved understanding of the various patterns of injury and shared similarities between different anatomical locations and physeal complexes.

Conflict of Interest
None declared.

References

1 Oestreich AE. The acrophysis: a unifying concept for understanding enchondral bone growth and its disorders. II. Abnormal growth. Skeletal Radiol 2004;33(03):119–128
2 Laor T, Jaramillo D. MR imaging insights into skeletal maturation: what is normal? Radiology 2009;250(01):28–38
3 Iannotti JP. Growth plate physiology and pathology. Orthop Clin North Am 1990;21(01):1–17
4 Brighton CT. The growth plate. Orthop Clin North Am 1984;15 (04):571–595
5 Rivas R, Shapiro F. Structural stages in the development of the long bones and epiphyses: a study in the New Zealand white rabbit. J Bone Joint Surg Am 2002;84(01):85–100
6 Nguyen JC, Markhardt BK, Merrow AC, Dwek JR. Imaging of pediatric growth plate disturbances. Radiographics 2017;37 (06):1791–1812
7 Caine DJ, Golightly YM. Osteoarthritis as an outcome of paediatric sport: an epidemiological perspective. Br J Sports Med 2011 Apr;45(04):298–303
8 Caine D, Maffulli N, Meyers R, Schöffl V, Nguyen J. Inconsistencies and imprecision in the nomenclature used to describe primary periphyseal stress injuries: towards a better understanding. Sports Med 2022;52(04):685–707
9 Blumer MJ, Longato S, Fritsch H. Structure, formation and role of cartilage canals in the developing bone. Ann Anat 2008;190(04): 305–315
10 Byers S, Moore AJ, Byard RW, Fazzalari NL. Quantitative histomorphometric analysis of the human growth plate from birth to adolescence. Bone 2000;27(04):495–501
11 Nguyen JC, Lee KS, Thapa MM, Rosas HG. US evaluation of juvenile idiopathic arthritis and osteoarticular infection. Radiographics 2017;37(04):1181–1201
12 Ogden JA. Injury to the growth mechanisms of the immature skeleton. Skeletal Radiol 1981;6(04):237–253
13 Jaimes C, Jimenez M, Marin D, Ho-Fung V, Jaramillo D. The trochlear pre-ossification center: a normal developmental stage and potential pitfall on MR images. Pediatr Radiol 2012;42(11):1364–1371
14 Aoyama JT, Maier P, Servaes S, et al. MR imaging of the shoulder in youth baseball players: anatomy, pathophysiology, and treatment. Clin Imaging 2019;57:99–109
15 Tomsan H, Grady MF, Ganley TJ, Nguyen JC. Pediatric elbow: development, common pathologies, and imaging considerations. Semin Roentgenol 2021;56(03):245–265
16 Ecklund K, Jaramillo D. Patterns of premature physeal arrest: MR imaging of 111 children. AJR Am J Roentgenol 2002;178(04): 967–972
17 Jaramillo D, Laor T, Hoffer FA, et al. Epiphyseal marrow in infancy: MR imaging. Radiology 1991;180(03):809–812
18 Jaramillo D, Kammen BF, Shapiro F. Cartilaginous path of physeal fracture-separations: evaluation with MR imaging—an experimental study with histologic correlation in rabbits. Radiology 2000;215(02):504–511
19 Rogers LF, Poznanski AK. Imaging of epiphyseal injuries. Radiology 1994;191(02):297–308
20 Jaramillo D, Shapiro F. Growth cartilage: normal appearance, variants and abnormalities. Magn Reson Imaging Clin N Am 1998;6(03):455–471
21 Thapa MM, Iyer RS, Khanna PC, Chew FS. MRI of pediatric patients: Part 1, normal and abnormal cartilage. AJR Am J Roentgenol 2012;198(05):W450–W455
22 Borsa JJ, Peterson HA, Ehman RL. MR imaging of physeal bars. Radiology 1996;199(03):683–687
23 Sailhan F, Chotel F, Guibal AL, et al. Three-dimensional MR imaging in the assessment of physeal growth arrest. Eur Radiol 2004;14(09):1600–1608
24 Smith BG, Rand F, Jaramillo D, Shapiro F. Early MR imaging of lower-extremity physeal fracture-separations: a preliminary report. J Pediatr Orthop 1994;14(04):526–533
25 Gabel GT, Peterson HA, Berquist TH. Premature partial physeal arrest. Diagnosis by magnetic resonance imaging in two cases. Clin Orthop Relat Res 1991;(272):242–247
26 Jaramillo D, Hoffer FA, Shapiro F, Rand F. MR imaging of fractures of the growth plate. AJR Am J Roentgenol 1990;155(06):1261–1265
27 Lohman M, Kivisaari A, Vehmas T, Kallio P, Puntila J, Kivisaari L. MRI in the assessment of growth arrest. Pediatr Radiol 2002;32 (01):41–45
28 Zbojniewicz AM, Laor T. Focal periphyseal edema (FOPE) zone on MRI of the adolescent knee: a potentially painful manifestation of

physiologic physeal fusion? AJR Am J Roentgenol 2011;197(04): 998–1004
29 Chan BY, Gill KG, Rebsamen SL, Nguyen JC. MR imaging of pediatric bone marrow. Radiographics 2016;36(06):1911–1930
30 Larson RL, McMahan RO. The epiphyses and the childhood athlete. JAMA 1966;196(07):607–612
31 Caine D, DiFiori J, Maffulli N. Physeal injuries in children's and youth sports: reasons for concern? Br J Sports Med 2006;40(09): 749–760
32 Flachsmann R, Broom ND, Hardy AE, Moltschaniwskyj G. Why is the adolescent joint particularly susceptible to osteochondral shear fracture? Clin Orthop Relat Res 2000;(381):212–221
33 Bailey DA, Wedge JH, McCulloch RG, Martin AD, Bernhardson SC. Epidemiology of fractures of the distal end of the radius in children as associated with growth. J Bone Joint Surg Am 1989; 71(08):1225–1231
34 Nguyen JC, Lin B, Potter HG. Maturation-dependent findings in the shoulders of pediatric baseball players on magnetic resonance imaging. Skeletal Radiol 2019;48(07):1087–1094
35 Alexander CJ. Effect of growth rate on the strength of the growth plate-shaft junction. Skeletal Radiol 1976;1(02):67–76
36 Xie M, Gol'din P, Herdina AN, et al. Secondary ossification center induces and protects growth plate structure. eLife 2020;9:9
37 DiFiori JP, Benjamin HJ, Brenner JS, et al. Overuse injuries and burnout in youth sports: a position statement from the American Medical Society for Sports Medicine. Br J Sports Med 2014;48 (04):287–288
38 Trueta J, Amato VP. The vascular contribution to osteogenesis. III. Changes in the growth cartilage caused by experimentally induced ischaemia. J Bone Joint Surg Br 1960;42-B:571–587
39 Laor T, Wall EJ, Vu LP. Physeal widening in the knee due to stress injury in child athletes. AJR Am J Roentgenol 2006;186(05): 1260–1264
40 Laor T, Hartman AL, Jaramillo D. Local physeal widening on MR imaging: an incidental finding suggesting prior metaphyseal insult. Pediatr Radiol 1997;27(08):654–662
41 Caine D, Meyers R, Nguyen J, Schöffl V, Maffulli N. Primary periphyseal stress injuries in young athletes: a systematic review. Sports Med 2022;52(04):741–772
42 Anderson M, Green WT, Messner MB. Growth and predictions of growth in the lower extremities. J Bone Joint Surg Am 1963;45-A:1–14
43 Beaty JH, Kumar A. Fractures about the knee in children. J Bone Joint Surg Am 1994;76(12):1870–1880
44 Allen H, Davis KW, Noonan K, Endo Y, Nguyen JC. Orthopaedic fixation devices used in children: a radiologist's guide. Semin Musculoskelet Radiol 2018;22(01):12–24
45 Sabick MB, Kim YK, Torry MR, Keirns MA, Hawkins RJ. Biomechanics of the shoulder in youth baseball pitchers: implications for the development of proximal humeral epiphysiolysis and humeral retrotorsion. Am J Sports Med 2005;33(11):1716–1722
46 Heyworth BE, Kramer DE, Martin DJ, Micheli LJ, Kocher MS, Bae DS. Trends in the presentation, management, and outcomes of Little League shoulder. Am J Sports Med 2016;44(06):1431–1438
47 Lin DJ, Wong TT, Kazam JK. Shoulder injuries in the overhead-throwing athlete: epidemiology, mechanisms of injury, and imaging findings. Radiology 2018;286(02):370–387
48 Albanese SA, Palmer AK, Kerr DR, Carpenter CW, Lisi D, Levinsohn EM. Wrist pain and distal growth plate closure of the radius in gymnasts. J Pediatr Orthop 1989;9(01):23–28
49 Caine D, Roy S, Singer KM, Broekhoff J. Stress changes of the distal radial growth plate. A radiographic survey and review of the literature. Am J Sports Med 1992;20(03):290–298
50 Jaramillo D, Laor T, Zaleske DJ. Indirect trauma to the growth plate: results of MR imaging after epiphyseal and metaphyseal injury in rabbits. Radiology 1993;187(01):171–178
51 Vender MI, Watson HK. Acquired Madelung-like deformity in a gymnast. J Hand Surg Am 1988;13(01):19–21
52 DiFiori JP, Puffer JC, Mandelbaum BR, Dorey F. Distal radial growth plate injury and positive ulnar variance in nonelite gymnasts. Am J Sports Med 1997;25(06):763–768
53 Longo UG, Ciuffreda M, Locher J, Maffulli N, Denaro V. Apophyseal injuries in children's and youth sports. Br Med Bull 2016;120(01): 139–159
54 Tariq SM, Patel V, Gendler L, et al. Pediatric thrower's elbow: maturation-dependent MRI findings in symptomatic baseball players. Pediatr Radiol 2023
55 Hodge C, Schroeder JD. Medial Epicondyle Apophysitis (Little League Elbow). StatPearls Available at: https://www.ncbi.nlm.nih.gov/books/NBK570592/ Accessed April 1, 2024
56 Hang DW, Chao CM, Hang YS. A clinical and roentgenographic study of Little League elbow. Am J Sports Med 2004;32(01):79–84
57 Kim HH, Gauguet JM. Pediatric elbow injuries. Semin Ultrasound CT MR 2018;39(04):384–396
58 Jacoby SM, Herman MJ, Morrison WB, Osterman AL. Pediatric elbow trauma: an orthopaedic perspective on the importance of radiographic interpretation. Semin Musculoskelet Radiol 2007;11 (01):48–56
59 Cole WW III, Brown SM, Vopat B, Heard WMR, Mulcahey MK. Epidemiology, diagnosis, and management of tibial tubercle avulsion fractures in adolescents. JBJS Rev 2020;8(04):e0186
60 Kushner RL, Massey P. Tibial Tubercle Avulsion. StatPearls Publishing; 2023 Available at: https://www.ncbi.nlm.nih.gov/books/NBK544275/ Accessed April 1, 2024
61 Pretell-Mazzini J, Kelly DM, Sawyer JR, et al. Outcomes and complications of tibial tubercle fractures in pediatric patients: a systematic review of the literature. J Pediatr Orthop 2016;36 (05):440–446
62 Kalifis G, Marin Fermin T, Seil R, Hobson S, Papakostas E, Hantes M. Tibial tubercle fractures are sports injuries in male adolescents with a considerable risk of complications and reoperations: a systematic review. Knee Surg Sports Traumatol Arthrosc 2023;31 (07):2624–2634
63 Ladenhauf HN, Seitlinger G, Green DW. Osgood-Schlatter disease: a 2020 update of a common knee condition in children. Curr Opin Pediatr 2020;32(01):107–112
64 Laor T, Zbojniewicz AM, Eismann EA, Wall EJ. Juvenile osteochondritis dissecans: is it a growth disturbance of the secondary physis of the epiphysis? AJR Am J Roentgenol 2012;199(05):1121–1128
65 Crawford DC, Safran MR. Osteochondritis dissecans of the knee. J Am Acad Orthop Surg 2006;14(02):90–100
66 Eismann EA, Pettit RJ, Wall EJ, Myer GD. Management strategies for osteochondritis dissecans of the knee in the skeletally immature athlete. J Orthop Sports Phys Ther 2014;44(09):665–679
67 Krause M, Hapfelmeier A, Möller M, Amling M, Bohndorf K, Meenen NM. Healing predictors of stable juvenile osteochondritis dissecans knee lesions after 6 and 12 months of nonoperative treatment. Am J Sports Med 2013;41(10):2384–2391
68 Hughes JA, Cook JV, Churchill MA, Warren ME. Juvenile osteochondritis dissecans: a 5-year review of the natural history using clinical and MRI evaluation. Pediatr Radiol 2003;33(06):410–417
69 Samora WP, Chevillet J, Adler B, Young GS, Klingele KE. Juvenile osteochondritis dissecans of the knee: predictors of lesion stability. J Pediatr Orthop 2012;32(01):1–4
70 Nguyen JC, Liu F, Blankenbaker DG, Woo KM, Kijowski R. Juvenile osteochondritis dissecans: cartilage T2 mapping of stable medial femoral condyle lesions. Radiology 2018;288(02): 536–543
71 O'Connor MA, Palaniappan M, Khan N, Bruce CE. Osteochondritis dissecans of the knee in children. A comparison of MRI and arthroscopic findings. J Bone Joint Surg Br 2002;84(02): 258–262
72 Kijowski R, Blankenbaker DG, Shinki K, Fine JP, Graf BK, De Smet AA. Juvenile versus adult osteochondritis dissecans of the knee: appropriate MR imaging criteria for instability. Radiology 2008; 248(02):571–578

73 Carey JL, Wall EJ, Grimm NL, et al; Research in OsteoChondritis of the Knee (ROCK) Group. Novel arthroscopic classification of osteochondritis dissecans of the knee: a multicenter reliability study. Am J Sports Med 2016;44(07):1694–1698
74 Turati M, Anghilieri FM, Bigoni M, et al. Osteochondritis dissecans of the knee: epidemiology, etiology, and natural history. J Child Orthop 2023;17(01):40–46
75 Logli AL, Bernard CD, O'Driscoll SW, et al. Osteochondritis dissecans lesions of the capitellum in overhead athletes: a review of current evidence and proposed treatment algorithm. Curr Rev Musculoskelet Med 2019;12(01):1–12
76 Kajiyama S, Muroi S, Sugaya H, et al. Osteochondritis dissecans of the humeral capitellum in young athletes: comparison between baseball players and gymnasts. Orthop J Sports Med 2017;5(03): 2325967117692513
77 Ellermann J, Johnson CP, Wang L, Macalena JA, Nelson BJ, LaPrade RF. Insights into the epiphyseal cartilage origin and subsequent osseous manifestation of juvenile osteochondritis dissecans with a modified clinical MR imaging protocol: a pilot study. Radiology 2017;282(03):798–806
78 Uozumi H, Sugita T, Aizawa T, Takahashi A, Ohnuma M, Itoi E. Histologic findings and possible causes of osteochondritis dissecans of the knee. Am J Sports Med 2009;37(10):2003–2008
79 Chau MM, Klimstra MA, Wise KL, et al. Osteochondritis dissecans: current understanding of epidemiology, etiology, management, and outcomes. J Bone Joint Surg Am 2021;103(12): 1132–1151
80 Matsui Y, Funakoshi T, Momma D, et al. Variation in stress distribution patterns across the radial head fovea in osteochondritis dissecans: predictive factors in radiographic findings. J Shoulder Elbow Surg 2018;27(05):923–930
81 Singer KM, Roy SP. Osteochondrosis of the humeral capitellum. Am J Sports Med 1984;12(05):351–360
82 Nguyen JC, Degnan AJ, Barrera CA, Hee TP, Ganley TJ, Kijowski R. Osteochondritis dissecans of the elbow in children: MRI findings of instability. AJR Am J Roentgenol 2019;213(05):1145–1151
83 Nguyen JC, Caine D. Youth soccer players: patterns of injury involving the primary growth plates of epiphyses. Skeletal Radiol 2024 Jan 4. Doi: 10.1007/s00256-023-04541-y. Epub ahead of print. PMID: 38175258